Structural Response
of an
Earth Covered Magazine
to a
Simulated Blast Loading

Joseph Hamilton [1], Mark Weaver [1], Joseph Abraham [1]

[1] Karagozian and Case, Inc. 700 N. Brand Ave, Suite 700, Glendale, CA 91203-3215

Abstract

A series of high-fidelity physics-based simulations were performed to assess the performance of an earth covered magazine (ECM) to an idealized airblast load applied to the soil above the roof. A representative ECM model was generated based on a survey of existing ECM drawing sets. The simulated structure consisted of reinforced concrete walls, columns with capitals and drop panels, and a roof slab. The concrete and soil were modeled using solid Lagrangian elements and the K&C concrete material model. Due to uncertainty regarding existing material strengths (i.e., due to variation in the surveyed drawing sets, age of these structures, and the limited amount of testing available for in-situ materials), unconfined concrete compressive strength and reinforcing steel yield strength were varied across the simulations performed.

This work records the assumptions inherent in the analytical model and the results obtained from these simulations. In particular, the ultimate failure modes observed and how failure modes changed as material properties were varied is presented. Based on the results of these simulations, recommendations concerning improvements to modeling ECMs are offered.

Introduction

Magazines are used for storing ammunition and explosive materials and they are classified as either Aboveground Magazines (AGM) or Earth Covered Magazines (ECM). As described in the Unified Facilities Criteria for Ammunition and Explosives Storage Magazines, an ECM is not designed to resist the effect of its own exploding contents. Rather the intended purpose of an ECM is to mitigate a sympathetic detonation from an adjacent ECM (U.S. Army Corps of Engineers 2015).

This paper provides a review of an effort to better understand the response of a representative ECM to a roof-applied airblast load and the model's sensitivity to material parameters such as concrete and reinforcing steel strength properties. The structure was modeled with LS-DYNA using Lagrangian elements and segment loading of the soil to simulate an airblast loading condition. To expedite run time, two versions of the ECM model were created. The first was a partial-strip model that was used to assess the sensitivity of the ECM's response to different loads and material strength properties. The second was a half-symmetry model that incorporated more realistic boundary conditions to better assess the ultimate failure mechanism of an ECM exposed to roof-applied airblast loads. The modeling setup and results from both the partial-strip and half-symmetry models is covered in this paper.

Model Setup

Three sets of drawings of ECMs from different time periods were reviewed to determine parameters for various properties of the building structure, such as concrete strength; reinforcing steel strength and layout; soil, wall and slab thicknesses; and column dimensions. In some cases, such as with wall thickness and reinforcing steel

layout, the values chosen were common to all drawing sets reviewed. However, in other cases, such as with the concrete and steel strengths, two values were chosen to bound the problem and assess how sensitive the response of the ECM was to these parameters.

The ECM is constructed of conventional reinforced concrete (RC) construction. The structure consists of two rows of columns with perimeter RC bearing walls that serve to create a six bay by three bay (of essentially equal size) single-story structure. Additionally, the structure was covered with approximately two feet of soil.

One concern from the outset was the CPU run time required to perform a simulation involving the full ECM. Thus, a partial-strip of the ECM was modeled for initial simulations. This partial-strip model, which consisted of a single line of columns as well as the roof slab tributary to these columns in the ECM's short direction, had an element count of 690,000. By contrast, the final half-symmetry ECM model had approximately 4.5 million elements. (A half-symmetry, rather than a the full, version of the ECM was possible because of the symmetrical layout of the building structure.) As a result, the partial-strip model allowed for a relatively rapid assessment of ECM sensitivity to various parameters and the load at which failure initiated. Once the loading range of interest was identified, additional simulations were performed using the half-symmetry model that incorporated more realistic boundary conditions. The partial strip and half-symmetry models are shown in Figure 1.
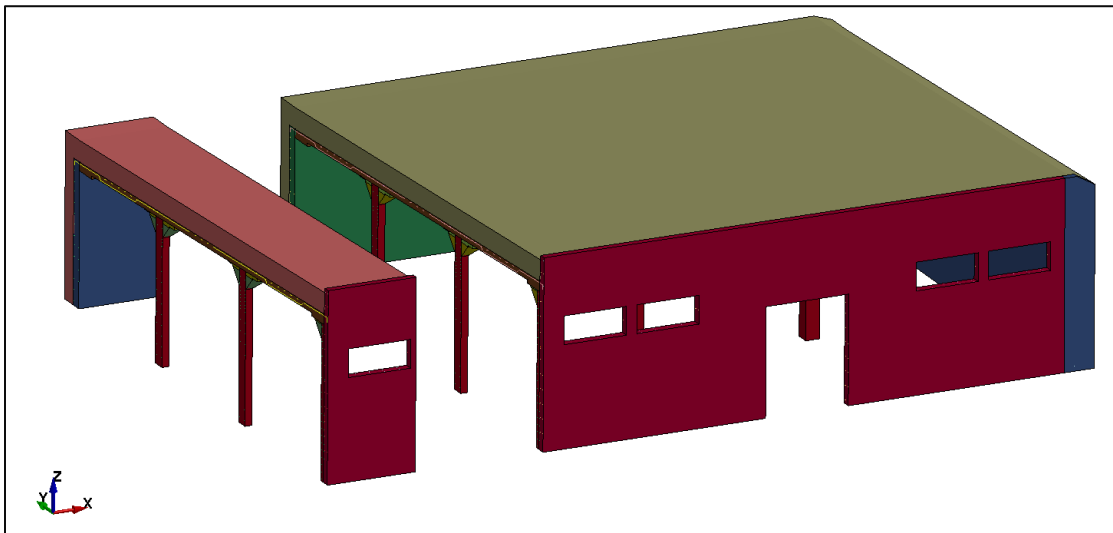

Figure 1. ECM analytical models (partial-strip model on left, half-symmetry model on right).

The reinforcing steel was modeled using beam elements with nodes co-localized (i.e., merged) with the concrete solid elements. The spacing and dimensions of the reinforcement was determined from the floor plans and each reinforcement bar was explicitly modeled. The lap splices were modeled by spacing the beam elements of one reinforcement bar on one side of a solid concrete element, and the other lapped bar was modeled on the other side of that concrete element. This placed a single concrete element between lap splices. Images of the reinforcing steel for the constitutive wall and roof panels are shown in Figure 2.
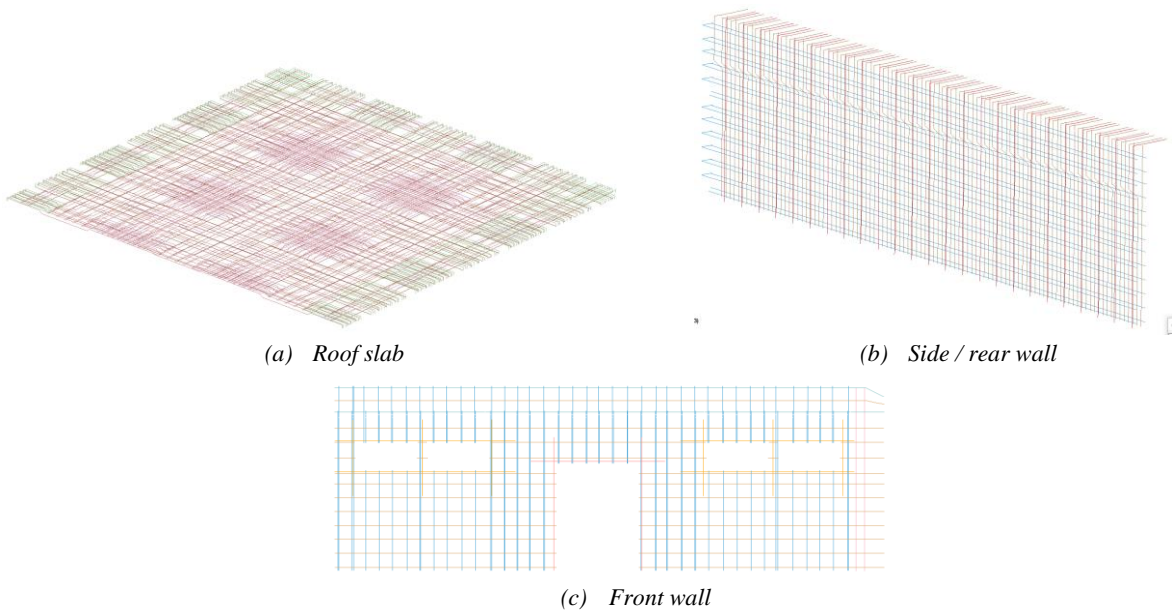
(a) Roof slab

(b) Side / rear wall

(c) Front wall

Figure 2. Reinforcing steel in roof slab, side/rear walls, and front wall.

Due to the geometry of the column capitals, and the difficulty of performing a mesh transition within the dimensional constraints, the CONTACT_TIED_NODES_TO_SURFACE keyword was used to transition certain areas of the mesh. Since the capital is part of the primary load path to the column, the geometry of the capital was not simplified or approximated. This accurate representation of the capital geometry helped ensure proper load transfer from the roof slab to the column over the duration of the simulation. The lower and upper portions of the capital, shown in Figure 3, required this CONTACT_TIED_NODES_TO_SURFACE transition approach. Additionally, the upper portion of the capital and the top of the column, shown in Figure 4 below, also required this mesh transition method.
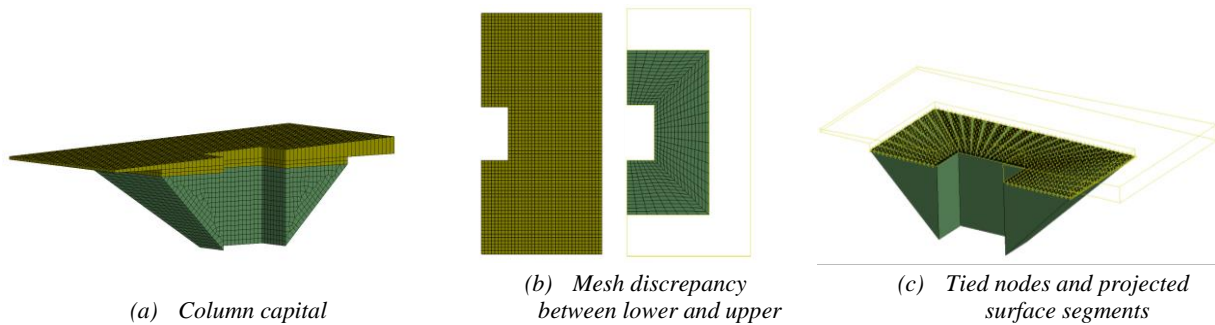

(a) Column capital

(b) Mesh discrepancy between lower and upper

(c) Tied nodes and projected surface segments

Figure 3. Column meshing transition between capital and drop section.

(a) Column and capital

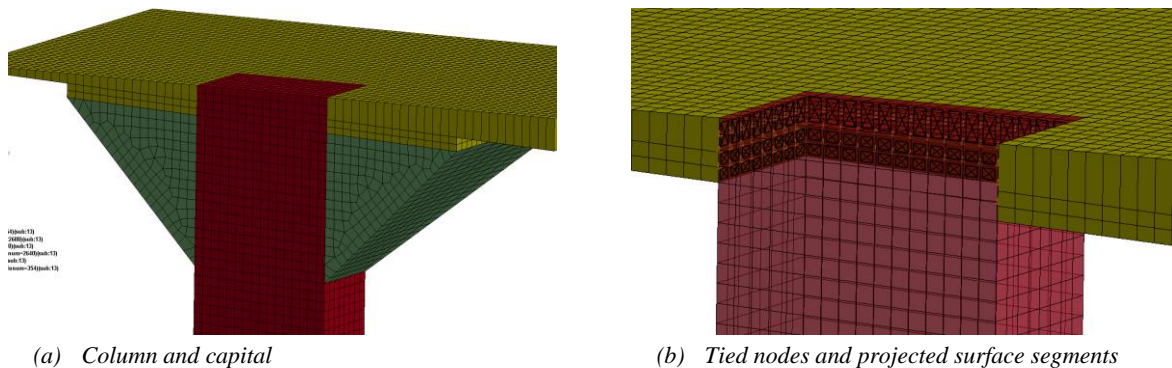*(b) Tied nodes and projected surface segments*

Figure 4. Capital and column attachment details.

The boundary conditions for both the partial-strip and half-symmetry models are shown in Figure 5. Symmetry constraints were applied along the centerline of the half-symmetry model, and on opposing faces of the partial-strip model. Fixed constraints were applied along all nodes on the base of the model. Additionally, rigid wall planes were placed along the outside of the soil in order to constrain the soil in compression without forming tension. A rigid wall plane was also placed at the base of the model to prevent debris from moving past the ground level. The stub portion of the retaining wall, only modeled in the half-symmetry model, was constrained as well.
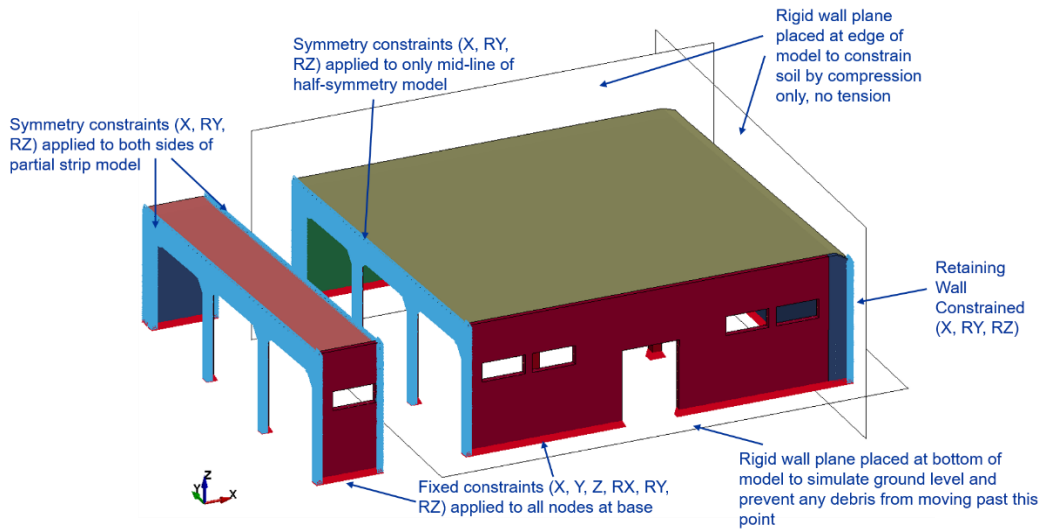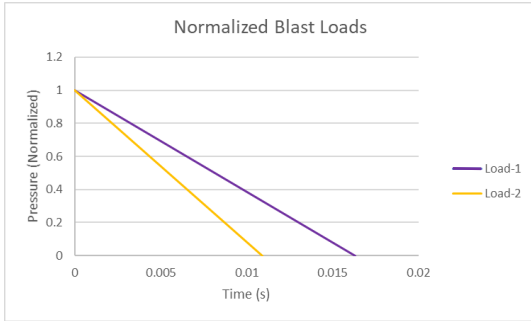

Figure 5. Boundary constraint details.

All concrete elements were modeled with LS-DYNA using hexahedra solid type 1 elements, and the average element dimensions were 1 inch by 1 inch by 1 inch. The material type chosen for the concrete was MAT_CONCRETE_DAMAGE_REL3 (MAT_072R3), which is a physics-based constitutive model suited for blast response calculations (Wu, et al. 2014). A lower bound unconfined compressive strength of concrete, f'_c, of 2,500 psi was indicated on the building plans and an upper bound f'_c of 8,000 psi was determined based on in-situ testing performed on ECM structures. The unconfined compressive strength of concrete was varied between simulation runs to assess ECM response sensitivity to concrete strength.
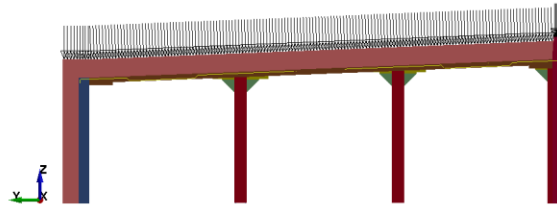
The soil was also modeled using hexahedra solid type 1 elements and MAT_072R3. The fit chosen for the soil material model was based on characterization tests for soil classified as silty sand with some gravel. The average dry bulk density of this soil was 114.9 pcf.

The reinforcing steel was modeled using beam elements and the LS-DYNA MAT_024 piecewise linear plasticity material model. Information from the building plans indicated the permissible tensile yield stress in reinforcement, f_s, was 20,000 psi. Per Section A.3.2 of ACI 318-89 (American Concrete Institute 1992), this f_s corresponds to either Grade 40 or Grade 50 reinforcement. As such, piecewise linear plasticity material models for both Grades 40 and 50 reinforcement were used. The specified yield strength of the reinforcing steel was varied between simulation runs to assess ECM response sensitivity to reinforcing steel strength.

At the outset of the simulation, a gravity load was ramped up over 400 ms and allowed to settle for 100 ms before the airblast load was applied. The loading of the structure was accomplished by applying a pressure history via load segments on the top of the soil. Two different simulated airblast loads were applied in separate simulations. The first was a load above the threshold for catastrophic structural failure in the model. The second load was below the first, and when applied to the structure there was either no collapse or late-time failure that initiated due to boundary instabilities. These loads will be referred to as Load-1 and Load-2, respectively. Both loads had the same peak pressure but different durations. Figure 6 shows the loads applied with the peak pressure normalized to one.

(a) Blast load curve shape example *(b) Load segments, with load applied in -Z direction*

Figure 6. Airblast load details.

Initial simulations involved the partial-strip model. This smaller model allowed for faster CPU run times, and the identification of critical load ranges for additional study. The concrete strengths of 2.5 ksi and 8.0 ksi were varied along with reinforcing steel strengths of 50 ksi and 40 ksi. A summary of the simulation runs performed and their material configurations are provided in Table 1.

Table 1. Simulation Run & Result Summary.

	Case	Concrete f'_c [ksi]	Rebar F_y [ksi]	Load	Result Summary
Partial Strip	P1	2.5	50	Load-1	Column crushing; roof slab collapse
	P2	2.5	50	Load-2	Late time column/wall rotation leads to structure collapse
	P3	2.5	40	Load-1	Column crushing; roof slab collapse
	P4	2.5	40	Load-2	Late time column/wall rotation leads to structure collapse
	P5	8	50	Load-1	Late time column/wall rotation leads to structure collapse
	P6	8	50	Load-2	No roof slab collapse
	P7	8	40	Load-1	Late time column/wall rotation leads to structure collapse
	P8	8	40	Load-2	No roof slab collapse
Half-Symmetry	H1	2.5	50	Load-1	Roof slab punching shear; roof slab collapse
	H2	2.5	50	Load-2	No roof slab collapse
	H5	8	50	Load-1	No roof slab collapse
	H6	8	50	Load-2	No roof slab collapse

Partial-Strip Results

The partial-strip model was initially used to identify loading thresholds and potential failure modes. In general, two modes of failure were observed in the partial-strip model. The first was observed later during simulation time and initialized by racking of the front and rear walls that resulted in element failure at the boundaries. The second was column crushing and subsequent roof slab collapse, which would occur relatively early in the simulation's run time. These typical failure mechanisms are shown below in Figure 7 (a) and (b), respectively. The boundary failure in (a) is seen specifically at the base of the walls and columns.
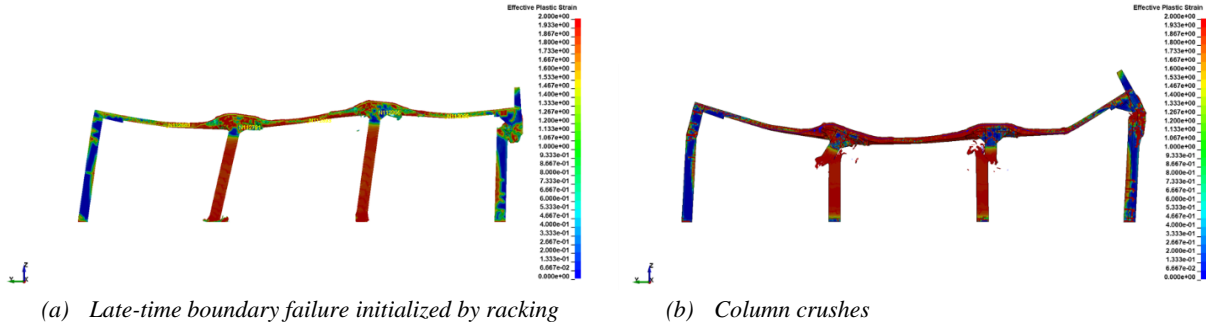
(a) Late-time boundary failure initialized by racking   *(b) Column crushes*

Figure 7. Partial-strip model failure modes.

The center node of the roof slab located at the midspan between columns was tracked for velocity. Stability after loading was identified by the node velocity returning to 0 in/s. This node velocity data is shown below in Figure 8 (a) and (b) for Load-1 and Load-2, respectively.
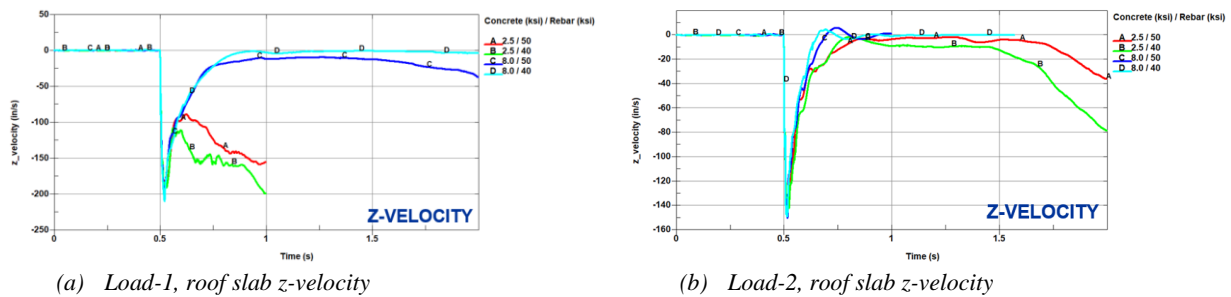

(a) Load-1, roof slab z-velocity   *(b) Load-2, roof slab z-velocity*

Figure 8. Partial-strip model roof slab velocity.

With the lower loading of Load-2, both 8.0 ksi concrete configurations using 40 ksi and 50 ksi steel showed stability. By contrast, both of the 2.5 ksi concrete configurations showed late time failure that was initialized by racking and resulted in structure collapse. This late-time failure indicated insufficient lateral resistance of the structure, which was an artifice of partial-strip modeling approach and boundary conditions.

With the higher load of Load-1, both cases using 2.5 ksi concrete had failure initialize with column crushing. Again, the late time racking of the structure that results in failure of the 8 ksi concrete case was attributed to the unrealistic boundary conditions of the partial-strip model. Both the Load-1 and Load-2 cases showed the structure response had greater sensitivity to concrete unconfined compressive strength than reinforcing steel yield strength. For this reason, the reinforcing steel specified stress was held constant at 50 ksi for the half-symmetry runs performed.

Half-Symmetry Results

The half-symmetry model introduced an additional wall into the model along the side of the structure. This side wall served to tie the front and rear walls together and also restrained them from moving inward. This "shear wall" provided resistance to and precluded the racking effects that were observed with the partial-strip model for all half-symmetry simulations performed.

During loading of the half-symmetry model, the restraint of the front and rear walls served to augment the tension force in the roof slab as evidenced by the damage contours shown in Figure 9 for case H1. In this simulation, starting at around 750 ms (i.e., shortly after the displacement responses of the two models started to diverge), the damage in the roof slab in the bays closest to the front and back walls is greater in the half-symmetry model than in the partial strip model. The end result of these effects was that a punching shear failure was observed in the half-symmetry model while a column crushing failure was observed with the partial-strip model. A screenshot showing this punching shear failure is included as Figure 10. For the remaining half-symmetry cases performed (i.e., cases H2, H5, and H6), no collapse mechanism was observed and the structure maintained its stability following the applied airblast load.
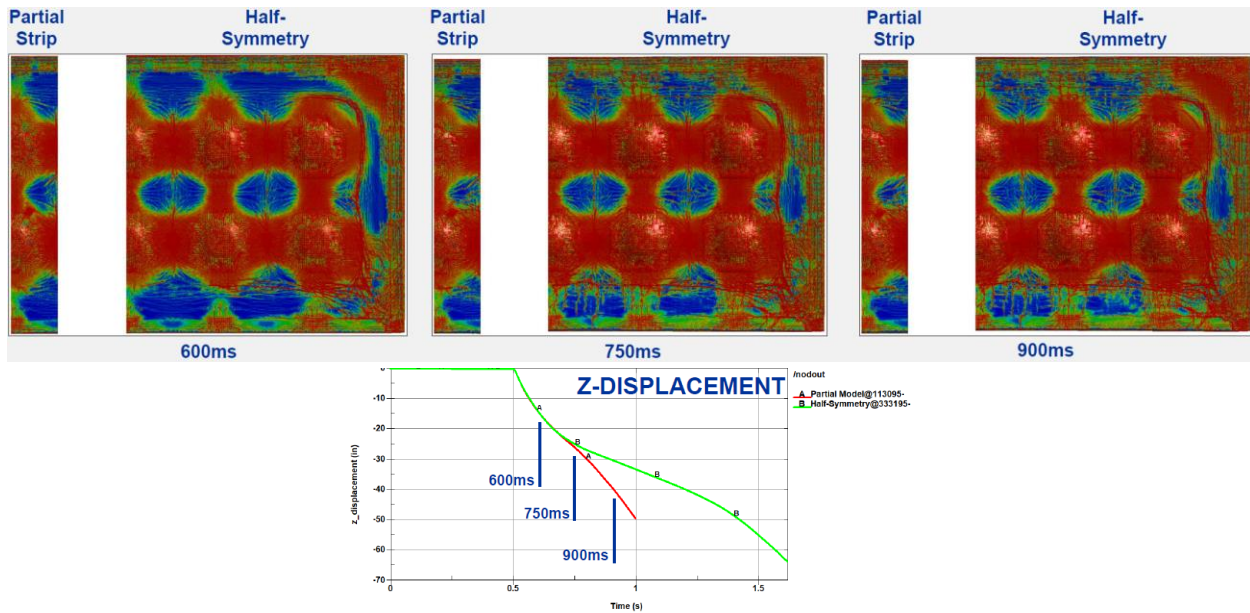
Approved for Public Release; Distribution Unlimited

Figure 9. Roof slab damage contours (plan view) at various times.
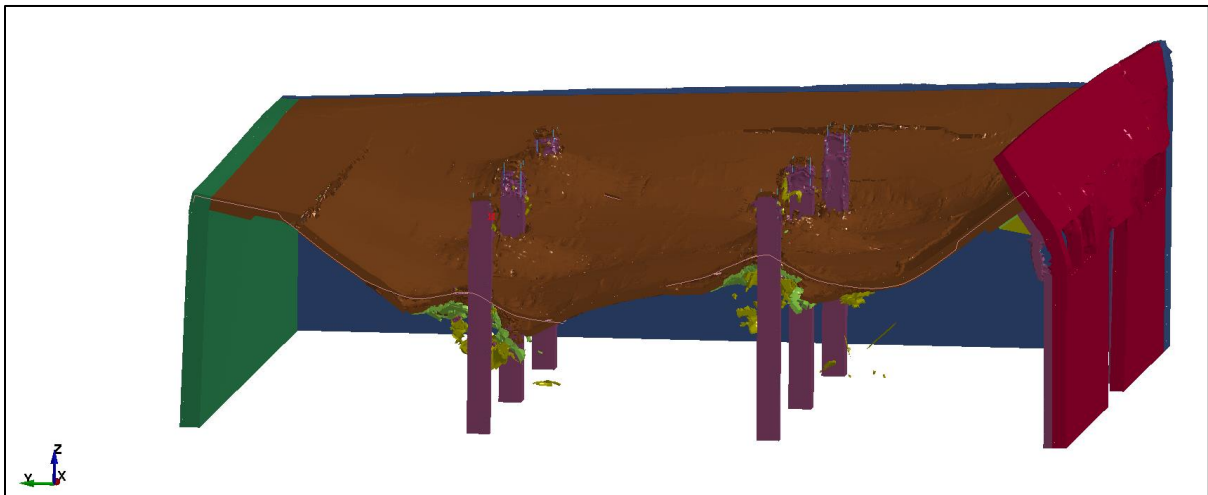

Figure 10. Punching shear failure in half-symmetry model.

As for the tracked nodal data with the partial-strip model, the centerline node located between the mid-span of the columns was tracked to provide roof slab velocity data. This data for the half-symmetry model is shown in Figure 11. The half-symmetry model results indicated stability for the lower loading condition, Load-2, with both 8.0 ksi and 2.5 ksi strength concrete. The higher Load-1 resulted in punching shear failure with 2.5 ksi strength concrete, but the 8.0 ksi concrete showed stability and no roof collapse.
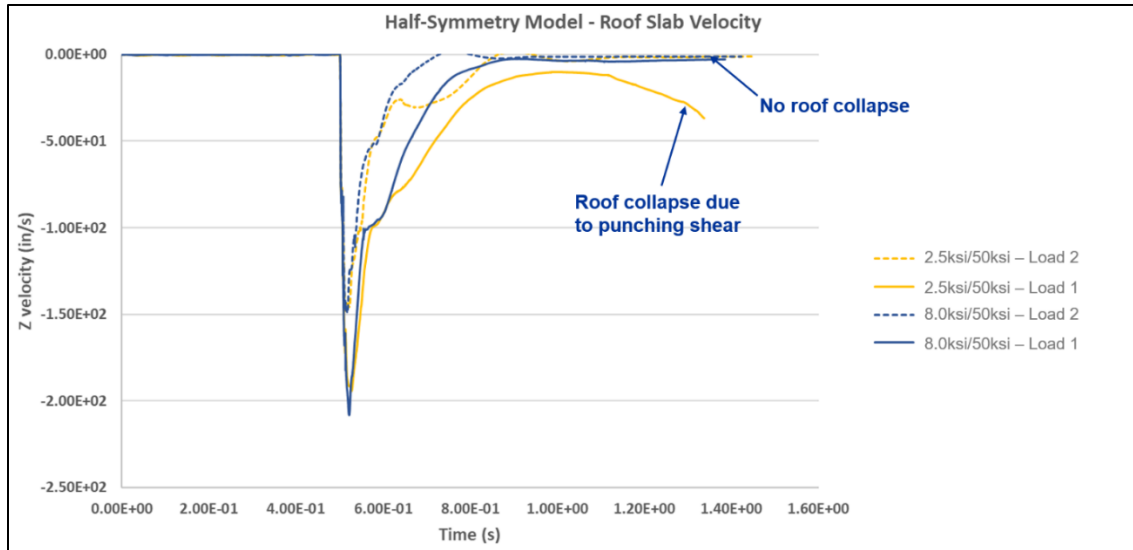
Figure 11. Half-symmetry model roof slab velocity.

Conclusions

High-fidelity physics-based calculations were performed to assess the response of a representative Earth Covered Magazine under two levels of external roof-applied blast load. A total of twelve simulations were performed in which the unconfined compressive strength of concrete was alternated between 2.5 ksi and 8.0 ksi and the specified yield strength of reinforcing steel was alternated between 40 ksi and 50 ksi. A partial-strip model that allowed for relatively short simulation times was used for initial studies to determine loading and material sensitivities. Final comparisons of identified critical material parameters were studied using a half-symmetry model.

The half-symmetry model showed punching shear failure of the roof slab while the partial-strip model showed column crushing as the initializing failure mechanism. This result indicates the importance of modeling the side wall in order to simulate more realistic boundary conditions when attempting to identify ultimate failure mechanisms for such structures where roof slab punching shear and column compression capacities are similar.

Additionally, with the particular ECM structure that was modeled, the structure stability was heavily dependent on the concrete strength. With 2.5 ksi concrete strength the structure showed stability with the lower Load-2 condition but exhibited collapse with the higher Load-1 condition whereas with the 8 ksi strength concrete stability was shown with both Load-1 and Load-2 conditions.

Acknowledgement

References

American Concrete Institute. 1992. "Building Code Requirements for Reinforced Concrete, ACI 318-89."
U.S. Army Corps of Engineers, Naval Facilities Engineering Command, Air Force Civil Engineer Center. 2015. "Unified Facilities Criteria - Ammunition and Explosives Storage Magazines."
Wu, Youcai, John E. Crawford, Shengrui Lan, and Joseph M. Magallanes. 2014. "Validation Studies for Concrete Constitutive Models with Blast Test Data." *13th International LS-DYNA Users Conference.* LSTC.